

Time-Series Contrastive Learning against False Negatives and Class Imbalance

Xiyuan Jin ¹, Jing Wang ^{1,2*}, Lei Liu ¹, Youfang Lin ^{1,2}

¹School of Computer and Information Technology, Beijing Jiaotong University, Beijing, China

²Beijing Key Laboratory of Traffic Data Analysis and Mining, Beijing, China

{xiyuanjin, wj, lei_liu, yflin}@bjtu.edu.cn;

Abstract

As an exemplary self-supervised approach for representation learning, time-series contrastive learning has exhibited remarkable advancements in contemporary research. While recent contrastive learning strategies have focused on how to construct appropriate positives and negatives, in this study, we conduct theoretical analysis and find they have overlooked the fundamental issues: **false negatives** and **class imbalance** inherent in the InfoNCE loss-based framework. Therefore, we introduce a straightforward modification grounded in the SimCLR framework, universally adaptable to models engaged in the instance discrimination task. By constructing instance graphs to facilitate interactive learning among instances, we emulate supervised contrastive learning via the multiple-instances discrimination task, mitigating the harmful impact of false negatives. Moreover, leveraging the graph structure and few-labeled data, we perform semi-supervised consistency classification and enhance the representative ability of minority classes. We compared our method with the most popular time-series contrastive learning methods on four real-world time-series datasets and demonstrated our significant advantages in overall performance.

Introduction

Benefiting from advancements in computational power and the availability of large-scale datasets, time-series-based deep learning has seen remarkable progress recently and finds extensive applications in disease diagnosis (Tang et al. 2021), traffic analysis (Guo et al. 2021), and financial prediction (Ding et al. 2015). However, annotating time-series in real-world scenarios poses unique challenges compared to other data types, such as images and videos, making large-scale dataset collection difficult. Specifically, in physiological time-series annotation, it is even necessary to involve multiple experts working collaboratively to ensure precise and reliable annotations (Gogolou et al. 2018).

As an important stepping stone towards generic representation learning without supervision, contrastive learning paradigms based on instance discrimination (Wu et al. 2018; Ye et al. 2019) demonstrated exceptional performance, even

surpassing current supervised methodologies across numerous tasks (He et al. 2020; Chen et al. 2020a). Its primary objective is to learn an encoder to discriminate positive pairs from negative pairs without any notion of semantic categories and end up with representations that capture apparent similarity among instances.

Inspired by such a strategy, time-series contrastive learning (TCL) methods have emerged and proposed various sample construction strategies tailored to time-series data with InfoNCE loss (Oord, Li, and Vinyals 2018), such as contrastive predictive coding (Oord, Li, and Vinyals 2018; Eldele et al. 2021), subseries discrimination (Franceschi, Dieuleveut, and Jaggi 2019), temporal neighborhood discrimination (Tonekaboni, Eytan, and Goldenberg 2021), etc. However, our in-depth theoretical analysis points out that current TCL methods still struggle with two fundamental challenges:

C1: How to alleviate the impact of false negatives under the instance discrimination task?

In the context of the instance discrimination task, unsupervised contrastive learning (UCL) often assumes manually designed augmentations or other views/modalities as positives, with the remaining samples within a mini-batch serving as negatives regardless of their semantic content (Chen et al. 2020a). Undoubtedly, this simple and efficient approach has greatly facilitated the widespread adoption of contrastive learning (Chen et al. 2020b; Li et al. 2021). However, ensuring the genuineness and effectiveness of negative samples remains a significant challenge. Without supervision, negative sample pairs are highly likely to consist of semantically similar or identical samples, which we refer to as false negatives. The existence of false negatives will severely impede the convergence of feature representation learning (Huynh et al. 2022; Zheng et al. 2021).

Recent works related to this question (Huynh et al. 2022) explored identifying false negatives and executing false negative elimination and attraction. However, the specific harmful impact of false negatives still lacks effective theoretical support, which motivates us to explore the theoretical basis and practicable solutions.

C2: How to improve the representation learning for highly imbalanced time-series classification?

Existing UCL methods typically operate agnostically to the distribution of training data. Nevertheless, time-series

*Corresponding author

This work has been submitted to the IEEE for possible publication. Copyright may be transferred without notice, after which this version may no longer be accessible.

data, particularly physiological time-series collected in real-world environments, often exhibit imbalanced distributions (Persley et al. 2019). This arises from the fact that disease occurrences typically endure shorter durations than non-disease periods, or some rare diseases inherently prevail less frequently than common ailments (Nattel 2002; Banerjee, Filippi, and Hauser 2009). Consequently, the availability of specific-class time-series data becomes inherently limited (Cao et al. 2013). Regrettably, the ability of most UCL methods would be declining for pivotal but infrequent minority classes (Zeng et al. 2023). Thus, a generic representation learning method and further research are needed.

Drawing inspiration from recent developments in supervised contrastive learning (SCL), this paper first theoretically analyzes the lower bound and dilemma of the InfoNCE loss in UCL. Then, we propose a *Semi-supervised Instance-graph-based Pseudo-Label Distribution Learning* framework (SIP-LDL) to mitigate the impact of false negatives while significantly improving the classification performance of minority classes. Specifically, we put forward a multiple-instances discrimination task to implement an approximation from UCL to SCL and further alleviate the impact of false negatives. Moreover, we propose to leverage an instance graph convolution to strengthen inter-instance relationships to replace the common-used linear projection head. Based on the feature propagation on the graph, we infer that the minority class suffers from more noisy neighbor instances than the majority leading to the feature underfitting, which motivated us to devise a semi-supervised consistency classification loss with minimal labeled samples to improve the loss and performance of the minority. In summary, our contributions can be summarized as follows:

- *New theoretical perspective*: we present a comprehensive theoretical analysis and derive the lower bound of contrastive loss to demonstrate the two primary challenges of UCL: **false negatives** and **class imbalance**, which implicitly deteriorates the quality of learned representations.
- *Simple and effective framework*: we introduce a novel SIP-LDL framework. Executing a multiple-instances discrimination task and propagating features on the instance graph, we alleviate the challenges of false negatives. Additionally, we employ a semi-supervised learning paradigm, utilizing a limited number of labeled samples to optimize the representative ability of minority classes.
- *Convincing results*: Extensive experiments demonstrate the effectiveness of our proposed model, surpassing the state-of-the-art on multiple physiological time-series datasets and achieving significant improvements, particularly for minority classes.

Related work

Contrastive Learning with Time-series

Various frameworks for contrastive learning have been proposed, which stem from the basic motivation of instance discrimination (Wu et al. 2018). Without relying on any se-

mantic supervisory information, instance-wise discrimination employs an encoder to strategically pull positives into closer alignment while concurrently enhancing the distinct separation among negatives. Subsequently, this process enhances the discriminative representation of each instance (Chen et al. 2020a). Expanding on this point, current time-series contrastive works study how to construct better positive pairs based on temporal invariance in time-series. For instance, CPC (Oord, Li, and Vinyals 2018) introduced a prediction-based context discrimination task to capture underlying shared information, followed by TSTCC (Eldele et al. 2021), which proposed cross-view discrimination with strong and weak augmentations. Additionally, TS2Vec (Yue et al. 2022) introduced fine-grained multi-scale context discrimination. Nevertheless, these approaches still exhibit limitations in guaranteeing the dissimilarity of chosen negative samples and fail to effectively tackle the problem of minority class feature underfitting in imbalanced datasets.

Contrastive Learning with False Negatives

False negative samples hinder the model’s effective convergence by forcing it to learn in the opposite direction of instances with similar or even identical semantics (Huynh et al. 2022; Zheng et al. 2021). Certain endeavors have sought to integrate analogous instances into model training to mitigate the repercussions stemming from false negatives. To illustrate, Zheng et al. (Zheng et al. 2021) construct a nearest neighbor graph for each instance within a mini-batch, subsequently deploying a KNN-based multicrop strategy to identify false negatives. More recently, Huynh et al. (Huynh et al. 2022) explored techniques for identifying false negatives without supervision and proceeded to explicitly eliminate detected instances or attract them as positives. In contrast, our approach involves utilizing samples from both the majority and minority classes with similar semantic traits to enhance learning rather than completely eliminate them.

Contrastive Learning with Class Imbalance

Learning discriminative representations on imbalanced datasets is a challenging task. Various methods have emerged to improve performance in the realm of imbalanced classification. Hybrid-PSC (Wang et al. 2021) introduces a novel hybrid network structure that combines contrastive learning with other techniques, leading to promising results. BCL (Zhu et al. 2022) presents a balanced contrastive loss that optimizes all classes for a balanced feature space, even in the presence of long-tail distributions. ImGCL (Zeng et al. 2023) utilizes the node centrality-based PBS method to automatically balance representations learned from GCL, which is particularly useful for graph-structured datasets. However, these methods either heavily rely on supervised information or are tailored to specific data types, such as graphs. Therefore our method presents a dedicated endeavor towards ameliorating class imbalance leveraging a cost-effective paradigm concurrently applicable across any data type.

Perspective

In the time-series classification task, we aim to learn a complex function φ mapping from an input space \mathcal{X} to the target space $\mathcal{Y} = [C] = \{1, 2, \dots, C\}$. The function φ is usually implemented as the composition of an encoder $f : \mathcal{X} \rightarrow \mathcal{H} \in \mathbb{R}^h$ and a linear classifier $W : \mathcal{H} \rightarrow \mathcal{Y}$. Usually, contrastive loss is applied on the embeddings Z after a projection $g : \mathcal{H} \rightarrow \mathcal{Z} \in \mathbb{R}^h$. Since the final classification accuracy strongly depends on the quality of the representations Z , we aim to learn an effective encoder f to improve representations against false negatives and class imbalance.

Next, we will give an in-depth analysis to point out the two major issues currently troubling UCL: **false negatives** and **class imbalance** from the differences in losses between SCL and UCL from a multi-class classification perspective.

Contrastive learning as Multi-Class classification

Given any two views, we can interpret contrastive learning as multi-class classification operating their representations (z_i, z_j) with a label 1 if it is sampled from the joint distribution $(i, j) \sim P_{ij}$, e.g., augmentations or other same-class samples, and -1 if it comes from the product of marginals, $(i, k) \sim P_i P_k$, e.g., other samples in a mini-batch. In the presence of false negatives, some negative pairs $(i, k) \sim P_i P_k$ should be labeled as positive.

Supervised and unsupervised contrastive loss. For an instance x_i of representation z_i in a batch B , supervised contrastive loss \mathcal{L}_{sc} and unsupervised contrastive loss \mathcal{L}_{uc} have the following expressions:

$$\mathcal{L}_{sc}(i) = -\frac{1}{|B_{y_i}| - 1} \sum_{j \in B_{y_i} \setminus \{i\}} \log \frac{\exp(z_i \cdot z_j / \tau)}{\sum_{k \in B \setminus \{i\}} \exp(z_i \cdot z_k / \tau)} \quad (1)$$

$$\mathcal{L}_{uc}(i) = -\log \frac{\exp(z_i \cdot z_j / \tau)}{\sum_{k \in B \setminus \{i\}} \exp(z_i \cdot z_k / \tau)} \quad (2)$$

where B_y is a subset of B that contains all samples of class y , $|\cdot|$ stands for the number of samples in the set, $\tau > 0$ is a scalar temperature hyperparameter. The UCL and SCL functions involve calculating expectations over either single or multiple positive pairs $(i, j) \sim P_{ij}$, along with independent negative pairs $(i, k) \sim P_i P_k$. Their mathematical formulation takes the shape of the $(|B| - 1)$ -way softmax cross-entropy loss. In SCL models, the ultimate objective revolves around classifying the nature of multiple same-class pairs $\{(z_i, z_j) | j \in \{B_{y_i} \setminus \{i\}\}\}$ as positives. In contrast, the UCL model focuses on the identification of the individual augmented pair (z_i, z_j) as positive.

It is worth mentioning that we do not distinguish between the negative sample size in SCL and UCL, although we usually select $2|B| - 2$ of the augmented samples as negatives with *NT-Xent* paradigm in UCL (Chen et al. 2020a), which does not exert any discernible influence on the ultimate analysis. Note that we will further omit τ and use $\langle z_i, z_j \rangle$ instead for calculating the similarity of embeddings z_i and z_j for simplicity.

We introduce the class-specific batch-wise loss as follows:

$$\mathcal{L}_{sc}(Z; Y, B, y) = \sum_{i \in B_y} \mathcal{L}_{sc}(i) \quad (3)$$

$$\mathcal{L}_{uc}(Z; Y, B, y) = \sum_{i \in B_y} \mathcal{L}_{uc}(i) \quad (4)$$

Two Main Drawbacks Analysis

In fact, previous work (Zhu et al. 2022) has demonstrated that existing SCL forms an undesired asymmetric geometry configuration for imbalanced datasets. In the following, we will give an in-depth analysis on UCL loss lower bound and prove that it leads to false negatives confliction as well as class imbalance issues homologous to the SCL loss.

Theorem 1. *Assuming the normalization function is applied for feature embeddings, let $Z = (z_1, \dots, z_N) \in \mathbb{Z}^N$ be an N point configuration with labels $Y = (y_1, \dots, y_N) \in [C]^N$, where $Z = \{z \in \mathbb{R}^h : \|Z\| = 1\}$. The class-specific batch-wise SCL loss \mathcal{L}_{sc} is bounded by:*

$$\mathcal{L}_{sc}(Z; Y, B, y) \geq \underbrace{\sum_{i \in B_y} \log(\underbrace{|B_y \setminus \{i\}|}_{\text{constant term}})}_{+} + \underbrace{|B_y^C| \exp\left(\frac{1}{|B_y^C|} \sum_{k \in B_y^C} \langle z_i, z_k \rangle - \frac{1}{|B_y| - 1} \sum_{j \in B_y \setminus \{i\}} \langle z_i, z_j \rangle\right)}_{\text{confrontation term}} \quad (5)$$

where we define B_y^C as the complement set of B_y .

The above lower bound of SCL loss is derived by (Graf et al. 2021), which consists of a *constant term* and a *confrontation term* redefined in our analysis. It means that the contrastive loss for class y depends on the size of y in the constant term and the size of its complement in the confrontation term that represents the confrontation between the mean representations of negative and positive sample pairs.

Furthermore, we have demonstrated in the Supplementary Material the differences in such losses between classes that the lower bound of SCL loss in the majority is much more than the minority, which leads to more beneficial gradient returns and better representations.

As shown in Figure 1, we discern that a relatively balanced dataset allows effective differentiation between majority and minority classes after sufficient learning of several epochs, as indicated by the higher losses experienced by the majority classes. However, a severely imbalanced dataset reveals a more troubling revelation: the loss of the majority class closely approximates that of the minority class. We infer that the class imbalance is exacerbated during learning, which leads to a greater loss decline of the majority while impeding the feature learning of the minority.

Theorem 2. *Let Z, Y be defined as in Theorem 1, the class-specific batch-wise UCL \mathcal{L}_{uc} loss is bounded by:*

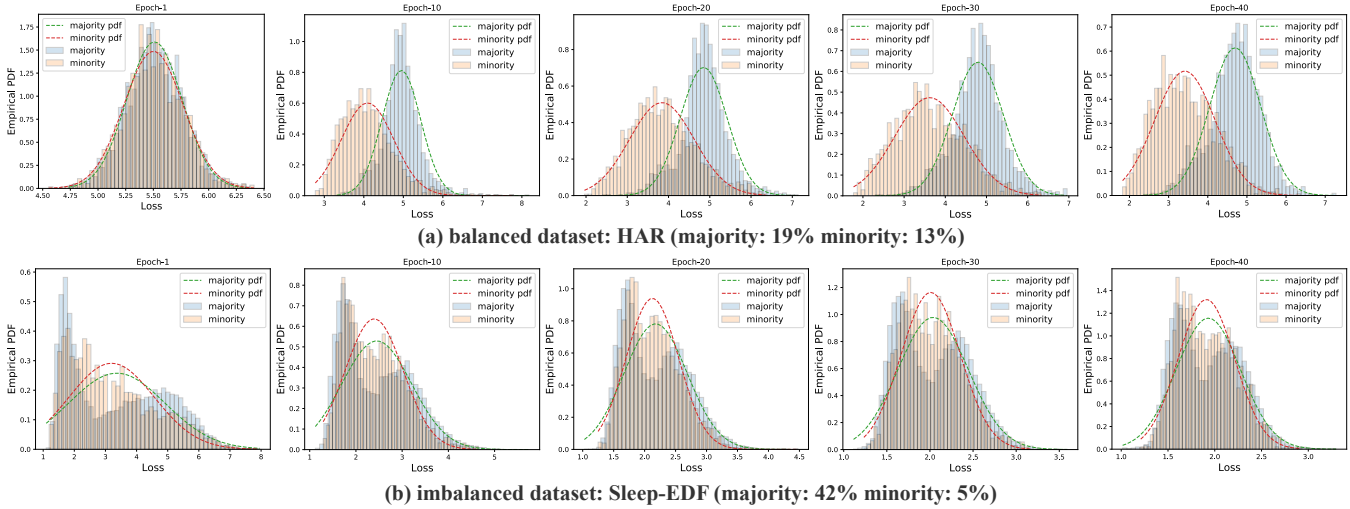


Figure 1: The loss distributions of the majority and minority on the balanced/imbalanced dataset as the training progresses.

$$\begin{aligned}
 \mathcal{L}_{\text{uc}}(Z; Y, B, y) \geq \sum_{i \in B_y} \log(& \\
 & \underbrace{|B_y \setminus \{i\}| \exp\left(\frac{1}{|B_y \setminus \{i\}|} \sum_{k \in |B_y \setminus \{i\}|} \langle z_i, z_k \rangle - \langle z_i, z_j \rangle\right)}_{\text{confliction term}} \\
 & + \underbrace{|B_y^C| \exp\left(\frac{1}{|B_y^C|} \sum_{k \in B_y^C} \langle z_i, z_k \rangle - \langle z_i, z_j \rangle\right)}_{\text{confrontation term}}) \\
 \end{aligned} \tag{6}$$

the *Proof*. has been provided in the Supplementary Material.

The differences between Equation (5) and Equation (6) are: 1) the *confliction term* replaces the *constant term*; 2) the mean of the positive sample representation $\frac{1}{|B_y|-1} \sum_{j \in B_y \setminus \{i\}} \langle z_i, z_j \rangle$ is replaced by $\langle z_i, z_j \rangle$.

Overall, the main drawbacks of UCL loss lie in:

- The exponential term in the *confliction term* indicates the learning conflict between false negative samples and positive pairs.
- The minority classes suffer from deficiencies in losses and gradients, which further leads to the feature underfitting homologous to SCL.

Method

To address the two key issues in UCL mentioned above, we propose a simple but effective SIP-LDL framework as an extension of SimCLR (Chen et al. 2020a).

The overall architecture of the SIP-LDL is shown in Figure 2. We propose to execute a multiple-instances discrimination task based on the single-instance discrimination task, which aims to implement an approximation from UCL to SCL and further alleviate the challenges of false negatives. Then, we replace the projection head from MLP to

GCN (Kipf and Welling 2016) to enhance feature interaction learning. On the one hand, instances of the majority can gain more substantial learning from same-class neighboring instances. On the other hand, losses of minority instances are enhanced through our semi-supervised consistency classification strategy as their features lack valid aggregation from scarce neighbor instances within the same class.

Multiple-Instances Discrimination

We get enlightenment from the loss form of SCL, which selects all instances of the same type in the entire mini-batch as positive samples to prevent the conflict of false negatives in the lower bound of SCL loss.

We aim to eliminate the gap between UCL and SCL as much as possible, which requires each instance to learn its corresponding pseudo-label distribution in the scenario of UCL. This means discovering other instances of the same type for each instance. Specifically, based on the previous analysis, the contrastive loss based on InfoNCE is equivalent to the cross-entropy loss, and the embedding similarity between each instance and the rest $|B| - 1$ samples can be used as the logical classification probability. Therefore, the goal of learning the distribution of instance pseudo labels is to discover and maximize the logical classification probability of potential samples of the same type, which is named multiple-instances discrimination in our study.

For a given time-series data, the pseudo-label distribution can be easily obtained by utilizing the similarity between samples. To be specific, for a given input time-series sample x_i , we generate an augmentation set \mathcal{T} through two separate augmentations (i.e., strong and weak augmentations) proposed by TSTCC (Eldele et al. 2021). Then, we feed its corresponding augmentations x_i^a into a contrastive encoder f_{enc} that maps samples to embeddings. We have $h_i = f_{\text{enc}}(x_i^a)$. Correspondingly, the logical classification probability $\alpha_{i,j}$ of sample x_i for category j (i.e., instance x_j) can be obtained from the following normalised similar-

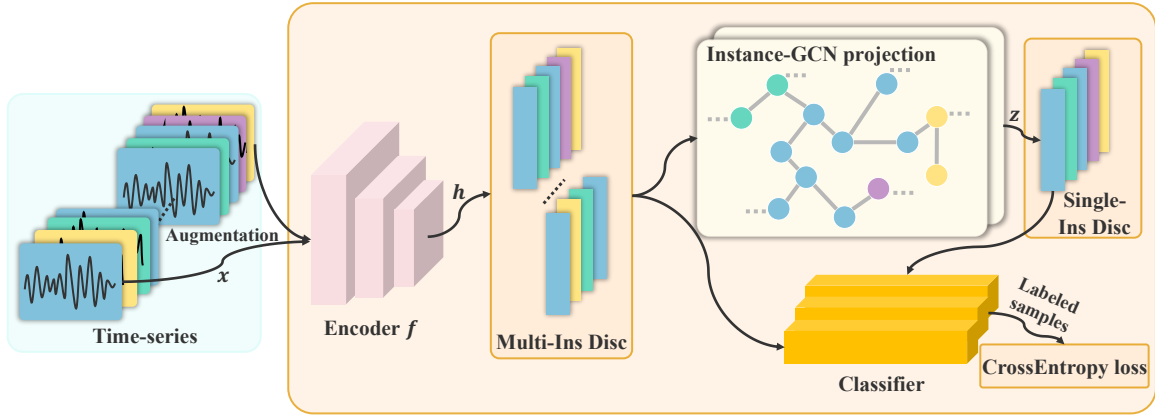


Figure 2: The overall architecture of the proposed SIP-LDL model.

ity:

$$\alpha_{i,j} = \frac{\exp(h_i \cdot h_j / \tau)}{\sum_{k \in B \setminus \{i\}} \exp(h_i \cdot h_k / \tau)} \quad (7)$$

Therefore, the multiple-instances discrimination loss of sample x_i is as follows:

$$\mathcal{L}_{\text{MID}}(i) = -\frac{1}{|B|-1} \sum_{j \in B \setminus \{i\}} \log \frac{\exp(h_i \cdot h_j / \tau)}{\sum_{k \in B \setminus \{i\}} \exp(h_i \cdot h_k / \tau)} \quad (8)$$

Instance Graph Convolution While MLPs are commonly employed as projection heads for mapping representations into the space where contrastive loss is applied, it is important to note that discriminating multiple instances often yields suboptimal outcomes. This is primarily due to the absence of a collaborative learning process among instances, which results in numerous erroneous relationships within the similarity matrix.

Therefore, we make simple modifications to the original architecture. We first construct the instance graph based on the similarity matrix in Equation (7), then replace MLP with GCN, which can greatly enhance the learning of correlation between instances without increasing any parameter or changing the model architecture. To be specific, the embeddings z_i of instance x_i can be obtained after two-layer spatial GCN projections are as follows:

$$z_i = \sum_{k \in B \setminus \{i\}} \alpha_{ij} (\sigma(\sum_{k \in B \setminus \{i\}} \alpha_{ij} h_{ij} W^{(1)})) W^{(2)} \quad (9)$$

where $\sigma(\cdot)$ denotes nonlinearity, $W^{(1)}$ and $W^{(2)}$ are weight matrices. To ensure that the learning of instance nodes can retain their own characteristics after being propagated on the graph, we still perform single-instance discrimination after the GCN projection:

$$\mathcal{L}_{\text{ID}}(i) = -\log \frac{\exp(z_i \cdot z_j / \tau)}{\sum_{k \in B \setminus \{i\}} \exp(z_i \cdot z_k / \tau)} \quad (10)$$

where z_i and z_j are embeddings of positive pairs, and z_i and z_k are embeddings of negative pairs.

Dataset	Train	Test	Length	Class	r_{im}
HAR	7352	2947	128	6	1.44
Sleep-EDF	25612	8910	3000	5	7.86
PhysioNet 2017	18256	5824	2500	4	24.97
TUSZ	1925	521	2400	4	40.34

Table 1: Description of datasets used in our experiments.

Semi-supervised Consistency Classification

As mentioned above, minority classes consistently struggle to obtain sufficient losses, regardless of whether in SCL or UCL, resulting in inadequate gradient assistance in learning representations.

Recently, SCL has shown promising performance in tackling imbalanced data through predefined class prototypes (Wang et al. 2021; Zhu et al. 2022), to further enable each class to have an approximate contribution for optimizing. Nevertheless, acquiring complete data labeling does not align with the prerequisites of those employing UCL methodologies. Furthermore, enhancing loss outcomes for minority groups within the context of entirely UCL empirically proves to be a formidable challenge (Sun et al. 2023). Therefore, we are driven to pursue a compromise approach: semi-supervised learning.

With a limited number of balanced labeled data, we train a classifier f_C with representations before and after graph convolution constraints as follows:

$$\mathcal{L}_C^h = -\sum_{l \in \mathcal{Y}_C} y_l \log(f_C(h_l)) \quad (11)$$

$$\mathcal{L}_C^z = -\sum_{l \in \mathcal{Y}_C} y_l \log(f_C(z_l)) \quad (12)$$

where \mathcal{Y}_C is the set of labeled instances, $\mathcal{L}_{CC} = \mathcal{L}_C^h + \mathcal{L}_C^z$ denotes the consistency classification loss.

The motivation behind our adoption of such a loss function stems from the realization that the minority class, following feature propagation on the graph, is inevitably susceptible to the influence of a multitude of noisy neighbor

Model Name	HAR		Sleep-EDF		PhysioNet 2017		TUSZ	
	Accuracy	F1-score	Accuracy	F1-score	Accuracy	F1-score	Accuracy	F1-score
Supervised	92.22 \pm 0.63	92.22 \pm 0.67	83.29 \pm 0.62	74.26 \pm 0.43	54.00 \pm 3.22	38.16 \pm 1.11	63.42 \pm 0.64	41.67 \pm 2.11
SCL	86.30 \pm 2.65	86.26 \pm 2.68	84.23 \pm 0.38	75.01\pm0.30	56.42 \pm 0.11	21.96 \pm 0.63	58.81 \pm 0.93	26.62 \pm 4.26
SimCLR	78.67 \pm 1.14	78.01 \pm 0.94	64.63 \pm 1.41	54.21 \pm 1.15	56.29 \pm 0.08	21.75 \pm 0.88	56.89 \pm 0.09	18.29 \pm 0.32
T-loss	79.51 \pm 3.49	78.78 \pm 3.83	80.53 \pm 0.78	70.15 \pm 0.32	54.27 \pm 0.84	37.15 \pm 0.51	62.03 \pm 0.53	38.07 \pm 0.96
CPC	68.56 \pm 3.04	68.32 \pm 3.22	62.68 \pm 2.62	47.71 \pm 3.10	54.46 \pm 1.27	38.83 \pm 0.52	61.77 \pm 0.43	36.41 \pm 0.71
TSTCC	88.31 \pm 1.00	88.31 \pm 1.02	81.41 \pm 0.55	70.53 \pm 0.29	56.52\pm1.02	40.48\pm0.50	60.73 \pm 1.03	35.36 \pm 3.98
TS2Vec	92.98 \pm 0.49	<u>93.01\pm0.50</u>	80.46 \pm 0.41	69.04 \pm 0.55	56.27 \pm 0.24	24.39 \pm 1.11	62.50 \pm 0.77	<u>42.26\pm1.61</u>
MLP+ \mathcal{L}_{ID}	79.95 \pm 1.73	81.28 \pm 1.70	65.28 \pm 1.57	57.49 \pm 2.97	56.17 \pm 0.09	22.22 \pm 0.89	56.78 \pm 0.19	18.11 \pm 0.04
MLP+ \mathcal{L}_{MID}	77.33 \pm 3.29	76.63 \pm 3.71	72.58 \pm 0.87	62.72 \pm 1.37	56.61 \pm 0.21	23.40 \pm 1.53	58.62 \pm 1.80	25.17 \pm 6.23
GCN+ \mathcal{L}_{ID}	59.95 \pm 2.01	56.74 \pm 2.02	41.08 \pm 2.28	24.57 \pm 1.69	56.01 \pm 0.47	20.71 \pm 0.49	57.08 \pm 0.09	18.49 \pm 0.40
GCN+ \mathcal{L}_{MID}	58.35 \pm 2.34	53.96 \pm 2.60	43.16 \pm 1.14	28.13 \pm 1.43	56.28 \pm 0.03	20.02 \pm 1.44	58.62 \pm 1.29	25.65 \pm 4.92
MLP+ \mathcal{L}_{MID} + \mathcal{L}_{ID}	80.48 \pm 2.09	79.51 \pm 2.23	75.86 \pm 1.63	64.80 \pm 1.49	56.74 \pm 0.20	25.50 \pm 0.83	59.58 \pm 1.42	29.92 \pm 5.63
GCN+ \mathcal{L}_{MID} + \mathcal{L}_{ID}	83.35 \pm 1.07	82.59 \pm 1.08	78.51 \pm 0.94	66.79 \pm 0.57	58.23 \pm 0.29	28.64 \pm 0.63	61.15 \pm 1.65	35.87 \pm 4.37
SIP-LDL	93.20\pm0.66	93.27\pm0.64	84.32\pm0.35	74.46\pm0.41	58.71\pm0.54	41.32\pm1.24	63.72\pm0.99	48.20\pm3.23

Table 2: Comparison between our proposed model against baselines using linear classifier evaluation experiment. The best results are marked in bold, the second-place results are underlined.

instances (i.e., majority classes), which resulted in suboptimal representations for the minority class. Therefore, the classification loss incurred on a uniformly sampled dataset inherently accentuates the loss experienced by the minority class, consequently engendering a more pronounced and effective gradient gain.

The final contrastive loss is the combination of the two multiple/single instance discrimination losses and the consistency classification loss as follows:

$$\mathcal{L} = \lambda_1 \cdot (\mathcal{L}_{MID} + \mathcal{L}_{ID}) + \lambda_2 \cdot \mathcal{L}_{CC} \quad (13)$$

where λ_1 and λ_2 are fixed scalar hyperparameters denoting the relative weight of each loss.

Experimental Setup

Datasets

To evaluate our model, we adopted 1 class-balanced dataset for human activity recognition and 3 class-imbalanced datasets for sleep stage classification, cardiac arrhythmia classification, and epileptic seizure classification, respectively. Detailed statistical information is summarized in Table 1. r_{im} denotes the ratio of class-imbalance.

Human Activity Recognition (HAR) We use UCI HAR dataset (Anguita et al. 2013), which contains sensor readings for 30 subjects performing 6 activities (i.e. walking, walking upstairs, downstairs, standing, sitting, and lying down).

Sleep Stage Classification (Sleep-EDF) We focus on Sleep Stage Classification, where we aim to categorize the input EEG signal into five classes: Wake (W), Non-rapid eye movement stages (N1, N2, N3), and Rapid Eye Movement (REM) stage (Goldberger et al. 2000). We used a single EEG channel (Fpz-Cz) with a sampling rate of 100 Hz.

Cardiac Arrhythmia Classification (PhysioNet 2017) PhysioNet 2017 (Clifford et al. 2017) consists of 8,528 single-lead ECG recordings alongside 4 different classes: Normal, Atrial Fibrillation, Other Rhythm, and Noisy.

Epilepsy Seizure Classification (TUSZ) The TUSZ dataset (Obeid and Picone 2016) comprises a total of 5,612 EEGs, with 3,050 annotated seizures, including 19 EEG channels and covering four distinct seizure types: combined focal (CF), generalized non-specific (GN), absence (AB), and combined tonic (CT) seizures (Tang et al. 2021).

Implementation Details

Experiments were repeated 5 times with 5 different seeds, and we reported the mean and standard deviation. The pre-training and downstream tasks were done for 40 epochs as we noticed that the performance did not improve with further training. We applied a batch size of 128. We used the Adam optimizer with a learning rate of 3e-4 and weight decay of 3e-4. We set $\lambda_1 = \lambda_2 = 1$. Lastly, we built our model using PyTorch 1.9 and trained it on an NVIDIA RTX A4000 GPU. We leverage 10% balanced labeled data to train semi-supervised consistency classification.

Results

Comparison with Baseline Approaches

We compare our proposed approach against the following baselines. (1) **Supervised**: supervised training of both encoder and classifier model; (2) **SCL**: supervised contrastive learning applied on SimCLR; (3) **SimCLR**; (4) **T-loss**; (5) **CPC**; (6) **TSTCC**; (7) **TS2Vec**. It is worth noting that we use strong and weak augmentations to adapt SimCLR to our application, as it was originally designed for images.

To evaluate the performance of our SIP-LDL, we follow the standard linear benchmarking evaluation scheme, which trains a linear classifier on top of a frozen pre-trained encoder. Table 2 shows the linear evaluation results of our approach against the baseline methods. Overall, our proposed SIP-LDL outperforms all five state-of-the-art methods on both class-balanced and imbalanced datasets while achieving comparable performance to the supervised approaches

on the Sleep-EDF dataset. This demonstrates the powerful representation learning capability of our model.

Ablation Study

To assess the individual contributions of each module in our scheme, we designed several variant models involving modifications to specific modules while keeping the rest of the architecture unchanged. In our study, we started by training a basic encoder+MLP model for the single-instance discrimination task referred to as $\text{MLP} + \mathcal{L}_{\text{ID}}$. Building on this, we replaced single-instance discrimination with multiple-instances discrimination, called $\text{MLP} + \mathcal{L}_{\text{MID}}$. Then, we replaced the MLP projection head with GCN, resulting in $\text{GCN} + \mathcal{L}_{\text{ID}}$ and $\text{GCN} + \mathcal{L}_{\text{MID}}$. Additionally, we simultaneously conducted multiple-instances discrimination for encoder representations and single-instance discrimination for projections, represented as $\text{MLP} + \mathcal{L}_{\text{MID}} + \mathcal{L}_{\text{ID}}$ and $\text{GCN} + \mathcal{L}_{\text{MID}} + \mathcal{L}_{\text{ID}}$ respectively. Finally, we trained the SIP-LDL model with \mathcal{L}_{CC} by incorporating a small amount of labeled data for consistency classification.

The results in Table 2 show that merely using multiple-instances discrimination did not consistently improve performance, likely due to limited interactions among instances. Introducing graph structures alone did not lead to significant improvements either. However, combining the instance graph and $\mathcal{L}_{\text{MID}} + \mathcal{L}_{\text{ID}}$ in our approach enhanced the model’s performance. Remarkably, by applying consistency classification \mathcal{L}_{CC} with only 10% of labeled data, we achieved substantial overall performance improvements.

Class Analysis

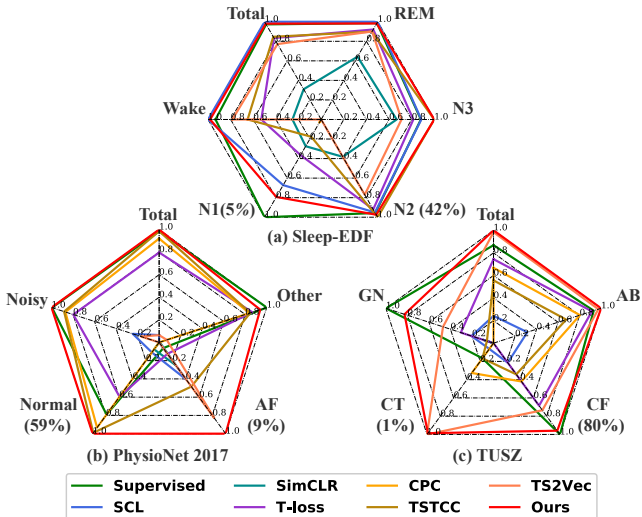


Figure 3: Normalized accuracy performance patterns of different sleep stages, cardiac arrhythmia types, and seizure types. The total and each class’s F1 scores were evaluated. The result of the method with the highest accuracy was recorded as 1. (a) Sleep-EDF dataset. (b) PhysioNet 2017 dataset, (c) TUSZ dataset.

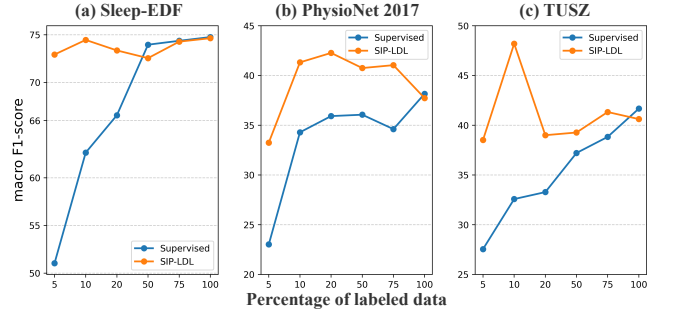


Figure 4: Comparison between supervised training vs. SIP-LDL for different few-labeled data scenarios in terms of MF1.

To assess the quality of the generated embeddings, we conducted a comparative analysis of SIP-LDL against supervised methods and five contrastive learning baselines on downstream classification tasks, with a specific focus on three class imbalance datasets. In Figure 3, we present a comprehensive comparison of overall classification F1 scores and F1 scores for each class, along with indicating the proportions of samples with the maximum and minimum amounts within each dataset.

Almost all the baseline methods perform poorly in the minority classes, while our SIP-LDL outperformed across all metrics, even surpassing supervised approaches in certain minority classes (e.g., AF in PhysioNet 2017 and CT in TUSZ). Compared to the classical SimCLR method based on the single-instance discrimination task, our proposed SIP-LDL strategy achieved substantial improvements in overall classification performance at the cost of limited labeled annotations.

Semi-supervised Training

We examined the effectiveness of SIP-LDL in a semi-supervised context. We trained the model with different percentages of labeled data: 5%, 10%, 20%, 50%, 75%, and 100%. SIP-LDL employs semi-supervised consistency classification, depicted by the orange curves in Figure 4. We found that supervised training struggles with limited labeled data. In contrast, our SIP-LDL method attains optimal results by employing a mere 10% of labeled data while concurrently rivaling the supervised method with 100% labeled data across three imbalanced datasets. While the supervised approach exhibit progressively improved performance with an increasing pool of available labeled instances, it is essential to underscore a notable divergence. Namely, when confronted with an escalation in labeled data, our SIP-LDL paradoxically experiences a performance decline. This phenomenon stems from the adverse effect of an enlarged label proportion on the integrity of our semi-supervised consistency classification framework. Consequently, the equilibrium among diverse sample classes is disrupted, leading to an encumbered learning process for the encoder and classifier, eventually succumbing to an imbalanced state.

Conclusion

We introduce a straightforward yet effective framework, SIP-LDL, to address the challenges of false negatives and class imbalance inherent in the single-instance discrimination task. Our proposed SIP-LDL employs a graph-based projection approach, imposing constraints on learning pseudo-label distributions for each instance, thereby approximating supervised contrastive learning. Simultaneously, we present a semi-supervised consistency classification loss, utilizing a mere 10% of annotated data, leading to substantial enhancements in minority classes. Remarkably, our framework can be seamlessly integrated into existing contrastive learning models for single-instance discrimination tasks without introducing additional model parameters.

References

Anguita, D.; Ghio, A.; Oneto, L.; Parra, X.; Reyes-Ortiz, J. L.; et al. 2013. A public domain dataset for human activity recognition using smartphones. In *Esann*, volume 3, 3.

Banerjee, P. N.; Filippi, D.; and Hauser, W. A. 2009. The descriptive epidemiology of epilepsy—a review. *Epilepsy research*, 85(1): 31–45.

Cao, H.; Li, X.-L.; Woon, D. Y.-K.; and Ng, S.-K. 2013. Integrated oversampling for imbalanced time series classification. *IEEE Transactions on Knowledge and Data Engineering*, 25(12): 2809–2822.

Chen, T.; Kornblith, S.; Norouzi, M.; and Hinton, G. 2020a. A simple framework for contrastive learning of visual representations. In *International conference on machine learning*, 1597–1607. PMLR.

Chen, T.; Kornblith, S.; Swersky, K.; Norouzi, M.; and Hinton, G. E. 2020b. Big self-supervised models are strong semi-supervised learners. *Advances in neural information processing systems*, 33: 22243–22255.

Clifford, G. D.; Liu, C.; Moody, B.; Li-wei, H. L.; Silva, I.; Li, Q.; Johnson, A.; and Mark, R. G. 2017. AF classification from a short single lead ECG recording: The PhysioNet/computing in cardiology challenge 2017. In *2017 Computing in Cardiology (CinC)*, 1–4. IEEE.

Ding, X.; Zhang, Y.; Liu, T.; and Duan, J. 2015. Deep learning for event-driven stock prediction. In *Twenty-fourth international joint conference on artificial intelligence*.

Eldele, E.; Ragab, M.; Chen, Z.; Wu, M.; Kwoh, C. K.; Li, X.; and Guan, C. 2021. Time-series representation learning via temporal and contextual contrasting. *arXiv preprint arXiv:2106.14112*.

Franceschi, J.-Y.; Dieuleveut, A.; and Jaggi, M. 2019. Unsupervised scalable representation learning for multivariate time series. *Advances in neural information processing systems*, 32.

Gogolou, A.; Tsandilas, T.; Palpanas, T.; and Bezerianos, A. 2018. Comparing similarity perception in time series visualizations. *IEEE transactions on visualization and computer graphics*, 25(1): 523–533.

Goldberger, A. L.; Amaral, L. A.; Glass, L.; Hausdorff, J. M.; Ivanov, P. C.; Mark, R. G.; Mietus, J. E.; Moody, G. B.; Peng, C.-K.; and Stanley, H. E. 2000. PhysioBank, PhysioToolkit, and PhysioNet: components of a new research resource for complex physiologic signals. *circulation*, 101(23): e215–e220.

Graf, F.; Hofer, C.; Niethammer, M.; and Kwitt, R. 2021. Dissecting supervised contrastive learning. In *International Conference on Machine Learning*, 3821–3830. PMLR.

Guo, S.; Lin, Y.; Wan, H.; Li, X.; and Cong, G. 2021. Learning dynamics and heterogeneity of spatial-temporal graph data for traffic forecasting. *IEEE Transactions on Knowledge and Data Engineering*, 34(11): 5415–5428.

He, K.; Fan, H.; Wu, Y.; Xie, S.; and Girshick, R. 2020. Momentum contrast for unsupervised visual representation learning. In *Proceedings of the IEEE/CVF conference on computer vision and pattern recognition*, 9729–9738.

Huynh, T.; Kornblith, S.; Walter, M. R.; Maire, M.; and Khademi, M. 2022. Boosting contrastive self-supervised learning with false negative cancellation. In *Proceedings of the IEEE/CVF winter conference on applications of computer vision*, 2785–2795.

Kipf, T. N.; and Welling, M. 2016. Semi-supervised classification with graph convolutional networks. *arXiv preprint arXiv:1609.02907*.

Li, Y.; Hu, P.; Liu, Z.; Peng, D.; Zhou, J. T.; and Peng, X. 2021. Contrastive clustering. In *Proceedings of the AAAI conference on artificial intelligence*, volume 35, 8547–8555.

Nattel, S. 2002. New ideas about atrial fibrillation 50 years on. *Nature*, 415(6868): 219–226.

Obeid, I.; and Picone, J. 2016. The temple university hospital EEG data corpus. *Frontiers in neuroscience*, 10: 196.

Oord, A. v. d.; Li, Y.; and Vinyals, O. 2018. Representation learning with contrastive predictive coding. *arXiv preprint arXiv:1807.03748*.

Perslev, M.; Jensen, M.; Darkner, S.; Jenum, P. J.; and Igel, C. 2019. U-time: A fully convolutional network for time series segmentation applied to sleep staging. *Advances in Neural Information Processing Systems*, 32.

Sun, W.; Zhang, J.; Wang, J.; Liu, Z.; Zhong, Y.; Feng, T.; Guo, Y.; Zhang, Y.; and Barnes, N. 2023. Learning Audio-Visual Source Localization via False Negative Aware Contrastive Learning. In *Proceedings of the IEEE/CVF Conference on Computer Vision and Pattern Recognition*, 6420–6429.

Tang, S.; Dunnmon, J. A.; Saab, K.; Zhang, X.; Huang, Q.; Dubost, F.; Rubin, D. L.; and Lee-Messer, C. 2021. Self-supervised graph neural networks for improved electroencephalographic seizure analysis. *arXiv preprint arXiv:2104.08336*.

Tonekaboni, S.; Eytan, D.; and Goldenberg, A. 2021. Unsupervised representation learning for time series with temporal neighborhood coding. *arXiv preprint arXiv:2106.00750*.

Wang, P.; Han, K.; Wei, X.-S.; Zhang, L.; and Wang, L. 2021. Contrastive learning based hybrid networks for long-tailed image classification. In *Proceedings of the IEEE/CVF*

conference on computer vision and pattern recognition, 943–952.

Wu, Z.; Xiong, Y.; Yu, S. X.; and Lin, D. 2018. Unsupervised feature learning via non-parametric instance discrimination. In *Proceedings of the IEEE conference on computer vision and pattern recognition*, 3733–3742.

Ye, M.; Zhang, X.; Yuen, P. C.; and Chang, S.-F. 2019. Unsupervised embedding learning via invariant and spreading instance feature. In *Proceedings of the IEEE/CVF conference on computer vision and pattern recognition*, 6210–6219.

Yue, Z.; Wang, Y.; Duan, J.; Yang, T.; Huang, C.; Tong, Y.; and Xu, B. 2022. Ts2vec: Towards universal representation of time series. In *Proceedings of the AAAI Conference on Artificial Intelligence*, volume 36, 8980–8987.

Zeng, L.; Li, L.; Gao, Z.; Zhao, P.; and Li, J. 2023. Imgcl: Revisiting graph contrastive learning on imbalanced node classification. In *Proceedings of the AAAI Conference on Artificial Intelligence*, volume 37, 11138–11146.

Zheng, M.; Wang, F.; You, S.; Qian, C.; Zhang, C.; Wang, X.; and Xu, C. 2021. Weakly supervised contrastive learning. In *Proceedings of the IEEE/CVF International Conference on Computer Vision*, 10042–10051.

Zhu, J.; Wang, Z.; Chen, J.; Chen, Y.-P. P.; and Jiang, Y.-G. 2022. Balanced contrastive learning for long-tailed visual recognition. In *Proceedings of the IEEE/CVF Conference on Computer Vision and Pattern Recognition*, 6908–6917.